Phosphorylation of PBX2, a novel downstream target of mTORC1, is determined by GSK3 and PP1

和田, 玲緒名

出版情報：Kyushu University, 2022, 博士（医学）, 課程博士
バージョン：

Regular Paper/Biochemistry

Phosphorylation of PBX2, a novel downstream target of mTORC1, is determined by GSK3 and PP1

Reona Wada[1], Shun Fujinuma[1], Hirokazu Nakatsumi[1], Masaki Matsumoto[1,2] and Keiichi I. Nakayama[1*]

[1]Department of Molecular and Cellular Biology, Medical Institute of Bioregulation, Kyushu University, 3-1-1 Maidashi, Higashi-ku, Fukuoka, Fukuoka 812-8582, Japan
[2]Department of Omics and Systems Biology, Graduate School of Medical and Dental Sciences, Niigata University, 757 Ichibancho, Asahimachi-dori, Chuo-ku, Niigata City, Niigata 951-8510, Japan

[*]*Correspondence:* Keiichi I. Nakayama, Department of Molecular and Cellular Biology, Medical Institute of Bioregulation, Kyushu University, 3-1-1 Maidashi, Higashi-ku, Fukuoka, Fukuoka 812-8582, Japan. Tel.:+81-92-642-6815. Fax: +81-92-642-6819. Email: nakayak1@bioreg.kyushu-u.ac.jp

Running head: Indirect PBX2 dephosphorylation by mTORC1

Abbreviations: DAPI, 4',6-diamidino-2-phenylindole; DMSO, dimethyl sulfoxide; ERK, extracellular signal–regulated kinase; FOXK1, forkhead box K1; GSK3, glycogen synthase kinase 3; HA, hemagglutinin; LARP1, La-related protein 1; MEK, ERK kinase; mTORC1, mechanistic target of rapamycin complex 1; PBS, phosphate-buffered saline; PBX2, pre–B cell leukemia transcription factor 2; PI3K, phosphoinositide 3-kinase; PDK1, phosphoinositide-dependent protein kinase 1; PP1, protein phosphatase 1; PP2A, protein phosphatase 2A; RAG, RAS-related GTP-binding protein; RHEB, Ras homolog enriched in Brain; shRNA, short hairpin RNA; siRNA, small interfering RNA; TBC1D7, TBC1 (TRE2-BUB2- CDC16) domain family member 7; TSC2, tuberous sclerosis complex 2; WT, wild-type.

Summary

Mechanistic target of rapamycin complex 1 (mTORC1) is a serine-threonine kinase that is activated by extracellular signals such as nutrients and growth factors. It plays a key role in the control of various biological processes such as protein synthesis and energy metabolism by mediating or regulating the phosphorylation of multiple target molecules, some of which remain to be identified. We have here reanalyzed a large-scale phosphoproteomics data set for mTORC1 target molecules and identified pre–B cell leukemia transcription factor 2 (PBX2) as such a novel target that is dephosphorylated downstream of mTORC1. We confirmed that PBX2, but not other members of the PBX family, is dephosphorylated in an mTORC1 activity–dependent manner. Furthermore, pharmacological and gene knockdown experiments revealed that glycogen synthase kinase 3 (GSK3) and protein phosphatase 1 (PP1) are responsible for the phosphorylation and dephosphorylation of PBX2, respectively. Our results thus suggest that the balance between the antagonistic actions of GSK3 and PP1 determines the phosphorylation status of PBX2 and its regulation by mTORC1.

Keywords: glycogen synthase kinase 3 (GSK3); mechanistic target of rapamycin complex 1 (mTORC1); pre–B cell leukemia transcription factor 2 (PBX2); phosphorylation; protein phosphatase 1 (PP1).

Mechanistic target of rapamycin complex 1 (mTORC1) is a serine-threonine kinase that regulates cellular responses to nutrient-related signals such as insulin and amino acids (1-3). Such signals activate mTORC1 on the cytoplasmic side of the lysosomal membrane (1,2,4), and the activated complex subsequently phosphorylates a variety of substrates, many of which regulate protein synthesis, autophagy, or metabolism to promote cell growth (1-3). Rapamycin, an inhibitor of mTORC1, has effects on cancer, immunity, and longevity (5-7), with these effects being largely dependent on attenuation of the mTORC1-mediated phosphorylation of downstream molecules. In addition to its classical function as a direct mediator of protein phosphorylation, recent studies including phosphoproteomics analyses have shown that mTORC1 also promotes dephosphorylation of downstream molecules in an indirect manner (8-11). We previously showed that dephosphorylation of the transcription factor FOXK1 (forkhead box K1) is regulated by mTORC1 and results in transcriptional activation of the gene for C-C chemokine ligand 2 (CCL2), an inflammatory chemokine that triggers the accumulation of monocytes and macrophages at sites of inflammation and thereby promotes tumor growth (9). Although mTORC1 plays a key regulatory role in various biological processes, many of its substrates remain to be identified, which has limited overall understanding of such regulation. The identification of novel targets of mTORC1 and elucidation of their mechanisms of action are expected to provide insight into complex molecular pathways subject to regulation by this kinase.

In the present study, we have reanalyzed our previously reported phosphoproteomics data obtained in a large-scale search for mTORC1 target molecules (9) and have identified pre–B cell leukemia transcription factor 2 (PBX2) as such a novel target. PBX proteins are transcription factors that belong to the highly conserved TALE (three amino acid loop extension) family, with four paralogs (PBX1, PBX2, PBX3, and PBX4) having been identified in human and mouse. PBX2 is expressed in a variety of tissues and is thought to regulate the expression of many genes as a homeobox cofactor that contributes to the control of development and cell differentiation (12-14). PBX2 is also highly expressed in many cancer types, with such high expression being associated with poor prognosis, especially in gastric cancer, esophageal squamous cell carcinoma, non–small cell lung cancer, and gingival squamous cell carcinoma (15-17). Indeed, depletion of PBX2 in gastric and esophageal squamous cell carcinoma cell lines was found to inhibit colony formation *in vitro* and

tumorigenicity *in vivo* (16). In gastric cancer, PBX2 interacts with homeobox A6 (HOXA6), which plays an important role in cancer growth and metastasis, with this interaction resulting in mutual protein stabilization and promotion of cancer migration and invasion (14). Given that mTORC1 is also abnormally activated in these cancer types and plays an important role in the proliferation and survival of the tumor cells (3,6,18-22), mTORC1-mediated regulation of PBX2 phosphorylation might contribute to their pathogenesis. The direct or indirect interaction between mTORC1 and PBX2 and the regulation of PBX2 phosphorylation state have not been investigated, however.

We now show that the phosphorylation state of PBX2 is dependent on mTORC1 activity, and that Ser^{330} of the mouse and human proteins is the target site for such phosphorylation. In contrast to a conventional target of mTORC1 action as a kinase, PBX2 was found to be dephosphorylated in response to mTORC1 activation. Pharmacological and gene knockdown experiments revealed that phosphorylation of PBX2 is indirectly regulated by mTORC1 and that glycogen synthase kinase 3 (GSK3) and protein phosphatase 1 (PP1) are responsible for PBX2 phosphorylation and dephosphorylation, respectively. Our results thus suggest that GSK3 and PP1 antagonistically regulate PBX2 phosphorylation downstream of mTORC1.

Materials and Methods

Antibodies, reagents, and cell culture

Antibodies for immunoblot analysis included those to the catalytic subunits of PP1 (clone E-9 monoclonal) obtained from Santa Cruz Biotechnology; those to PBX2 (polyclonal) from Atlas Antibodies; those to HSP90 (polyclonal) from Enzo Life Sciences; those to p70 S6 kinase (clone 49D7), to phospho–p70 S6 kinase (clone 108D2 monoclonal), to 4E-BP1 (clone 53H11 monoclonal), to phospho–4E-BP1 (polyclonal), to S6 (clone 5G10 monoclonal), to phospho-S6 (polyclonal), to GSK3α/β (clone D75D3 monoclonal), to AKT (polyclonal), to phospho-AKT (clone D9E monoclonal), to ERK1/2 (polyclonal), to phospho-ERK1/2 (polyclonal), to MAPKAPK-2 (polyclonal), to phospho–MAPKAPK-2 (clone 27B7 monoclonal), and to the catalytic subunits of PP2A (clone 52F8 monoclonal) from Cell Signaling Technology; and those to the HA.11 epitope tag (clone 16B12 monoclonal) from BioLegend. Immunocytofluorescence analysis was performed with the same antibodies to GSK3α/β and to the catalytic subunits of PP1 as well as with antibodies to the hemagglutinin

(HA) epitope tag (clone C29F4 monoclonal) obtained from Cell Signaling Technology. Rapamycin was obtained from LC Laboratories; Torin 1 and Go6983 from Tocris Bioscience; calyculin A from Cell Signaling Technology; LY294002, AZD6244, SB203580, and SB216763 from Selleck Chemical; AktVIII from Sigma-Aldrich; staurosporine from Wako Pure Chemical Industries; and CHIR99021 from Axon. 3T3-L1 and HeLa cells were checked for mycoplasma contamination with the use of MycoAlert (Lonza), and they were cultured under an atmosphere of 5% CO_2 at 37°C in Dulbecco's modified Eagle's medium (DMEM) supplemented with 10% fetal bovine serum, 1 mM sodium pyruvate, 2 mM L-glutamine, nonessential amino acids (10 ml/l, Invitrogen), 2-mercaptoethanol (50 μM), and antibiotics. The cells were maintained in medium containing a reduced serum concentration of 0.1% for 16 h before stimulation with 100 nM insulin.

Retrovirus expression system

Complementary DNAs encoding mouse PBX1, PBX2, PBX3, or PBX4, each with a COOH-terminal HA epitope tag, were subcloned into pMX-puro (kindly provided by T. Kitamura, The University of Tokyo, Japan) with the use of a NEBuilder HiFi DNA Assembly system (New England Biolabs). The resulting vectors were introduced into Plat-E packaging cells by transfection in order to generate recombinant retroviruses. 3T3-L1 cells were infected with the retroviruses in the presence of polybrene (5 μg/ml) and were then cultured in the presence of puromycin (5 μg/ml) for selection.

RNA interference

Small interfering RNAs (siRNAs) specific for human PP1 catalytic subunits A (s10930), B (s10933), or C (s719) or for PP2A catalytic subunits A (s10957) or B (s10960), as well as Silencer Select Negative Control #1 as a control, were obtained from Thermo Fisher Scientific. Cells were transfected with the siRNAs with the use of Lipofectamine RNAiMAX (Invitrogen). A retroviral vector (pCX4/Hygromycin) for expression of short hairpin RNAs (shRNAs) was described previously (23), and 3T3-L1 cells were depleted of GSK3α and GSK3β with the use of a modified shRNA (miR-E) system. The target sequences were 5′-ACCCTTGGACAAAGGTGTTCAA-3′ (nucleotides 1276–1297) for mouse GSK3α, 5′-ACCGATCTGTCTTGAAGAAATA-3′ (nucleotides 1312–1333) for mouse GSK3β, and 5′-ACCGCCTGAAGTCTCTGATTAA-3′ (nucleotides

1309–1330) for firefly luciferase as a control. The shRNA vectors were introduced into Plat-E cells for generation of recombinant retroviruses, and 3T3-L1 cells were infected with the retroviruses in the presence of polybrene (5 μg/ml) and were then cultured in the presence of hygromycin B (300 μg/ml) for selection.

Immunoblot analysis

Cells were washed with ice-cold phosphate-buffered saline (PBS), lysed in a lysis buffer [50 mM Tris-HCl (pH 7.5), 150 mM NaCl, 0.5% Triton X-100, 4 mM sodium orthovanadate, 4 mM EDTA, 100 mM NaF, 100 mM sodium pyrophosphate, 1 mM phenylmethylsulfonyl fluoride, protease inhibitor cocktail (Complete, Roche)], and fractionated by SDS-PAGE on a 10% gel or on an 8% gel supplemented with 50 μM Phos-tag (NARD Institute) and 10 μM $MnCl_2$. Divalent cations were removed from Phos-tag gels after electrophoresis by incubation twice for 5 min with transfer buffer containing 1 mM EDTA.

Immunofluorescence analysis

Cells were fixed for 10 min with 4% paraformaldehyde in PBS, washed three times with PBS, and incubated overnight at 4°C in staining buffer [0.45% Triton X-100 and 1% BSA fraction V (Roche) in PBS] containing primary antibodies. They were then washed three times with PBS before incubation for 30 min at room temperature with Alexa Fluor 488–conjugated secondary antibodies (Invitrogen) in staining buffer. Nuclei were stained with 4',6-diamidino-2-phenylindole (DAPI). The cells were examined with a laser-scanning confocal microscope (LSM700, Carl Zeiss, or BZ-X800, Keyence).

Statistical analysis

Quantitative data are presented as means ± SEM and were analyzed with Dunnett's test as performed with Rstudio software. A P value of <0.05 was considered statistically significant.

Results

Identification of PBX2 as a downstream effector of mTORC1

To identify new targets of mTORC1 that are dephosphorylated in response to mTORC1

activation, we first reanalyzed large-scale phosphoproteomics data obtained in our previous study (9) for HeLa cells subjected to various conditions that activate mTORC1 including stimulation with serum, insulin, or amino acids (Fig. 1A). A total of 75 proteins was found to be dephosphorylated in response to serum stimulation in a manner sensitive to rapamycin but not to U0126, an inhibitor of the extracellular signal–regulated kinase (ERK) kinase MEK. In addition, 1480 and 319 proteins were dephosphorylated in response to insulin or amino acid stimulation, respectively, in a time-dependent manner. Eleven of these various proteins were commonly dephosphorylated under all three conditions, and among these proteins only PBX2, FOXK1, and La-related protein 1 (LARP1) underwent dephosphorylation at the same sites under all three conditions (Fig. 1B). Given that FOXK1 (9,11,24,25) and LARP1 (26) were already known to be regulated downstream of mTORC1, we focused on the mechanism underlying regulation of the phosphorylation of PBX2, which had not been previously identified as a downstream effector of mTORC1, in the present study.

mTORC1-dependent dephosphorylation of PBX2

We next performed Phos-tag SDS-PAGE to detect changes in the phosphorylation state of PBX2. In this approach, the interaction of the phosphate groups of phosphorylated proteins with Phos-tag slows protein migration rate, allowing the separation of phosphorylated and nonphosphorylated forms of a given protein without the use of phospho-specific antibodies (27). Immunoblot analysis after Phos-tag SDS-PAGE revealed that the electrophoretic mobility of the immunoreactive band corresponding to PBX2 was increased in response to insulin stimulation in 3T3-L1 cells (Fig. 2A), suggestive of PBX2 dephosphorylation. This mobility shift was greatly attenuated by treatment of the cells with the mTORC1 inhibitors rapamycin or Torin 1, indicative of its dependence on mTORC1 activation. Furthermore, only PBX2 among the four paralogs of the PBX family showed a change in electrophoretic mobility in response to mTORC1 activation (Fig. 2B). These results thus suggested that PBX2 is a novel target for mTORC1 activity–dependent dephosphorylation.

Ser^{330} of PBX2 is dephosphorylated in the nucleus

Our phosphoproteomics analysis revealed that Ser^{330} of PBX2 was dephosphorylated in an mTORC1-dependent manner (Fig. 1B). To validate this result biochemically, we

generated 3T3-L1 cells expressing a mutant (S330A) of PBX2 in which Ser^{330} is replaced by Ala and which mimics the Ser^{330}-dephosphorylated form of the protein. Phos-tag SDS-PAGE and immunoblot analysis revealed that the electrophoretic mobility of the S330A mutant was not affected by the activation state of mTORC1 and was similar to that of wild-type (WT) PBX2 in cells stimulated with insulin (Fig. 3A), consistent with the notion that Ser^{330} of PBX2 is dephosphorylated in response to mTORC1 activation. We also generated 3T3-L1 cells expressing mutants (S330D and S330E) of PBX2 in which Ser^{330} is replaced by Asp or Glu and which mimic the Ser^{330}-phosphorylated form of the protein. Phos-tag SDS-PAGE and immunoblot analysis revealed that the electrophoretic mobility of the S330D mutant was also not affected by mTORC1 activation status and was similar to that of the S330A mutant, suggesting that Asp did not interact with Phos-tag.

PBX2 and mTORC1 differ in their subcellular localizations, with the former localizing predominantly to the nucleus (28) and the latter to the cytoplasm (29). Given that PBX2 is dephosphorylated in an mTORC1-dependent manner, we examined whether its subcellular localization might be dependent on its phosphorylation state. However, immunocytofluorescence staining revealed that WT and S330A, S330D, and S330E mutant forms of PBX2 were all localized to the nucleus in 3T3-L1 cells (Fig. 3B). Consistent with this observation, the subcellular localization of PBX2(WT) was not affected by treatment of cells with rapamycin, Torin 1, or insulin (Fig. 3C and D), suggesting that PBX2 localizes to the nucleus regardless of the phosphorylation state of Ser^{330}. Together, our results thus indicated that PBX2 dephosphorylation occurs in the nucleus as a result of an indirect action of mTORC1, and that signaling between mTORC1 in the cytoplasm and PBX2 in the nucleus may be mediated by some unidentified factor.

mTORC1 regulates PBX2 phosphorylation through GSK3

Our finding that Ser^{330} of PBX2 is phosphorylated in cells in which mTORC1 is inactive suggested the presence of another kinase that phosphorylates PBX2. To identify such a kinase, we examined the effects of various kinase inhibitors on the phosphorylation of PBX2 at Ser^{330} in 3T3-L1 cells exposed to both insulin and Torin 1. Treatment of the cells with staurosporine, a broad-spectrum kinase inhibitor, attenuated the signal intensity of the band corresponding to Ser^{330}-phosphorylated PBX2 and

increased that of the band corresponding to the Ser^{330}-dephosphorylated protein in a concentration-dependent manner (Fig. 4A). On the other hand, inhibitors of phosphatidylinositol 3-kinase (LY294002) and AKT (AktVIII), both of which function upstream of mTORC1, had no effect on the phosphorylation state of PBX2. Given that insulin-stimulated phosphorylation of Ser^{473} of AKT was shown to be mediated by mTORC2 (30), Torin 1 treatment inhibited the phosphorylation of Ser^{473} of AKT. We also found that a protein kinase C inhibitor (Go6983) partially inhibited Ser^{330}-phosphorylation of PBX2, whereas inhibitors of MEK (AZD6244) and p38 mitogen-activated protein kinase (SB203580) had no effect on PBX2 phosphorylation status (Fig. 4B). In contrast, inhibitors of GSK3 (SB216763 and CHIR99021) were found to reduce the signal intensity of the band corresponding to Ser^{330}-phosphorylated PBX2 and to increase that of the band corresponding to the Ser^{330}-dephosphorylated protein in a concentration-dependent manner (Fig. 4B and C). Consistent with these results, shRNA-mediated depletion of GSK3α or GSK3β in 3T3-L1 cells attenuated the phosphorylation of PBX2 at Ser^{330}, and this effect was more pronounced in cells depleted of both GSK3α and GSK3β (Fig. 4C).

Given that inhibition of mTORC1 has been shown to result in the nuclear accumulation of GSK3 and consequent phosphorylation by GSK3 of its substrates in the nucleus (24), we performed immunocytofluorescence staining to examine the subcellular localization of GSK3 in serum-deprived 3T3-L1 cells exposed to insulin with or without rapamycin or Torin 1. Activation of mTORC1 by insulin stimulation was associated with translocation of GSK3 from the nucleus to the cytoplasm, whereas inhibition of mTORC1 activity by rapamycin or Torin 1 attenuated this effect (Fig. 4D). Overall, these results suggested that mTORC1 regulates the nuclear-cytoplasmic translocation of GSK3, and that suppression of mTORC1 activity promotes the nuclear accumulation of GSK3 and consequent phosphorylation of PBX2 at Ser^{330}.

PP1 dephosphorylates PBX2 at Ser^{330}

To identify intervening molecules that mediate dephosphorylation of PBX2 in response to mTORC1 activation, we examined several candidate phosphatases. Given that the serine-threonine protein phosphatases PP1 and PP2A are responsible for >90% of protein phosphatase activity in eukaryotic cells (31), we focused on these enzymes and examined whether calyculin A, which inhibits the activity of both PP1 and PP2A, might

suppress mTORC1-dependent PBX2 dephosphorylation. Treatment of serum-deprived 3T3-L1 cells with calyculin A inhibited in a concentration-dependent manner the change in the electrophoretic mobility of PBX2 induced by insulin stimulation (Fig. 5A). We also found that siRNA-mediated depletion of the catalytic subunits of PP1 in HeLa cells increased the signal intensity of the band corresponding to Ser^{330}-phosphorylated PBX2 relative to that of the band corresponding to the Ser^{330}-dephosphorylated protein under both basal and insulin-stimulated conditions (Fig. 5B and C). In contrast, depletion of the catalytic subunits of PP2A did not affect the signal intensity of the bands corresponding to Ser^{330}-phosphorylated or Ser^{330}-dephosphorylated PBX2 in the absence or presence of insulin stimulation (Fig. 5B and C), suggesting that PP2A may not contribute to PBX2 dephosphorylation at this site. In addition, depletion of the catalytic subunits of PP2A resulted in an increase in the signal intensity of a band with the highest mobility shift, which likely represents a hyper-dephosphorylated form of PBX2. Although the mechanism underlying this phenomenon is unclear, one possible explanation is that the depletion of the catalytic subunits of PP2A might result in up-regulation of activity or expression level of the other protein phosphatases such as PP1 that target PBX2, through an unknown compensatory mechanism. Another possibility is that PP2A activates some kinases that phosphorylate PBX2, and that the depletion of the catalytic subunits of PP2A might result in inactivation of such kinases, leading to an increase in the amount of non-phosphorylated forms of PBX2. Given the difference in mobility of the bands, phosphorylation of PBX2 likely occurs at multiple residues other than Ser^{330}. Dephosphorylation of PBX2 at Ser^{330} was also observed under conditions of simultaneous inhibition of GSK3 and mTORC1 (Fig. 4A and C), suggesting that PP1 might mediate dephosphorylation of PBX2 at Ser^{330} in an mTORC1 activity–independent manner.

The catalytic subunits of PP1 show a broad tissue and subcellular distribution, with their subcellular localization being dynamically altered by interaction with various proteins (31,32). We found that the catalytic subunits of PP1 were localized to the nucleus of 3T3-L1 cells both under the basal condition and after stimulation with insulin in the absence of presence of rapamycin or Torin 1 (Fig. 5D). These results thus suggested that the subcellular localization of PP1 is independent of insulin stimulation and thus of mTORC1 activity in these cells.

Discussion

We have here shown that PBX2 undergoes dephosphorylation at Ser^{330} in an mTORC1 activity–dependent manner, consistent with the reanalysis of our phosphoproteomics data implicating PBX2 as a novel target molecule for mTORC1. Furthermore, immunofluorescence staining of cells expressing phosphomimetic or dephosphomimetic Ser^{330} mutants of PBX2 revealed that PBX2 localizes to the nucleus regardless of its phosphorylation state. Consistent with this finding, we also showed that PBX2(WT) localizes to the nucleus independently of mTORC1 activity. Our results thus suggest that phosphorylation of PBX2 is regulated in the nucleus.

The serine-threonine kinase GSK3 has two paralogs, GSK3α and GSK3β, in mammals and is known to phosphorylate >100 substrates important for the regulation of cell growth and metabolism. The activity of GSK3α is regulated predominantly by phosphorylation at Ser^{21} (inhibiting) and Tyr^{279} (activating), with Ser^{9} and Tyr^{216} being the corresponding residues targeted for regulation in GSK3β. GSK3 is active in cells under basal conditions and is inactivated by inhibitory phosphorylation in response to cell stimulation by hormones or growth factors (33). Furthermore, mTORC1 inhibition by rapamycin treatment has been shown to promote redistribution of GSK3 from the cytoplasm to the nucleus and thereby to affect phosphorylation of GSK3 substrates, but it did not alter the phosphorylation state of Ser^{21} of GSK3α and Ser^{9} of GSK3β (24,34). This scenario is consistent with our experimental results showing that phosphorylation of PBX2 at Ser^{330} is mediated by GSK3 that accumulates in the nucleus in cells in which mTORC1 is inactive. Similarly, the phosphorylation state of GSK3 might not be affected by mTORC1 activation as was the case for previous studies.

Protein serine-threonine phosphatases PP1 and PP2A generally form holoenzymes consisting of multiple functionally distinct subunits. In particular, the regulatory subunits have been shown to determine the catalytic activity, substrate specificity and subcellular localization of such phosphatases (35,36). Given that both PP1 and PP2A contain catalytic and regulatory subunits, the latter likely regulates their binding specificity to the substrates including PBX2. PP1 regulates diverse cellular processes through substrate dephosphorylation and is composed of a catalytic subunit and a variety of regulatory subunits, with the interaction of these subunits having been shown to control substrate specificity and localization of the holoenzyme (31,32). For example, PPP1R3B, a regulatory subunit of PP1 that contributes to the regulation of

blood glucose clearance and glycogen synthesis in the liver, associates with and thereby promotes the dephosphorylation of glycogen synthase in response to its own phosphorylation by insulin-activated AKT (37). We found that PP1 mediated the dephosphorylation of PBX2 at Ser^{330} and was localized to the nucleus of cells in a manner independent of mTORC1 activity.

We have demonstrated in the present study that mTORC1 regulates the phosphorylation state of PBX2 by controlling the subcellular localization of GSK3. Given that insulin stimulation activates the PI3K-PDK1-AKT axis upstream of mTORC1 (1,4), this pathway is possibly one of the key signals that regulate mTORC1-GSK3–mediated PBX2 phosphorylation. On the other hand, as shown in a previous study (37), it is also possible that the insulin-AKT axis directly regulates PP1 phosphatase activity in an mTORC1-GSK–independent manner. However, our results have shown that insulin stimulation no longer affects the phosphorylation state of PBX2 at Ser^{330} in the context of complete GSK3 depletion, suggesting that the GSK3-independent insulin-AKT-PP1 axis minimally contributes to the regulation of PBX2 phosphorylation state. Together with a number of supportive data showing that PBX2 is dephosphorylated in an mTORC1 activation–dependent manner, we concluded that the mTORC1-mediated regulation of GSK3 localization predominantly determines the phosphorylation state of PBX2, downstream of nutrient-related signals such as insulin.

There are several limitations to our study. First, although we examined by multiple approaches the roles of GSK3 and PP1 in PBX2 phosphorylation and dephosphorylation, respectively, it remains possible that GSK3 and PP1 actually regulate other downstream kinases and phosphatases that directly determine the phosphorylation status of PBX2. Second, whereas 3T3-L1 cells (mouse) were used for most experiments, HeLa cells (human) were used to examine the effects of PP1 and PP2A depletion, given that 3T3-L1 cells manifested marked growth inhibition in response to such depletion. On the other hand, our results indicate that mTORC1-dependent regulation of PBX2 phosphorylation is conserved between these two species, suggesting that it may play an important role *in vivo*.

Activation of mTORC1 regulates many biological processes including translation, autophagy, metabolism, and cell proliferation, not only through direct phosphorylation of key substrates but also through inhibition of the phosphorylation of numerous other targets. Given that mTORC1 is abnormally activated in many cancer

types (3-6, 18-22) and PBX2 is highly expressed in many cancer types (15-17), mTORC1 likely promotes the progression of these cancers by altering the stability of PBX2 as a protein and transcriptional activities such as PBX2 DNA binding affinity and binding ability to co-factors through the regulation of PBX2 phosphorylation status. Such biological aspects of PBX2 phosphorylation regulation in normal as well as cancer cell contexts await future study.

Acknowledgements

We thank T. Akagi for the pCX4 system; S. Mise, T. Higa, and other laboratory members for discussion; as well as A. Ohta for help with preparation of the manuscript.

Conflict of Interest Statement

The authors have no conflicts of interest to declare.

References

1. Shimobayashi, M., and Hall, M. N. (2014) Making new contacts: the mTOR network in metabolism and signalling crosstalk. *Nat. Rev. Mol. Cell Biol.* **15**, 155-162
2. Liu, G. Y., and Sabatini, D. M. (2020) mTOR at the nexus of nutrition, growth, ageing and disease. *Nat. Rev. Mol. Cell Biol.* **21**, 183-203
3. Cornu, M., Albert, V., and Hall, M. N. (2013) mTOR in aging, metabolism, and cancer. *Curr Opin Genet Dev* **23**, 53-62
4. Gonzalez, A., and Hall, M. N. (2017) Nutrient sensing and TOR signaling in yeast and mammals. *EMBO J.* **36**, 397-408
5. Lushchak, O., Strilbytska, O., Piskovatska, V., Storey, K. B., Koliada, A., and Vaiserman, A. (2017) The role of the TOR pathway in mediating the link between nutrition and longevity. *Mech. Ageing Dev.* **164**, 127-138
6. Li, J., Kim, S. G., and Blenis, J. (2014) Rapamycin: one drug, many effects. *Cell Metab.* **19**, 373-379
7. Elloso, M. M., Azrolan, N., Sehgal, S. N., Hsu, P. L., Phiel, K. L., Kopec, C. A., Basso, M. D., and Adelman, S. J. (2003) Protective effect of the immunosuppressant sirolimus against aortic atherosclerosis in apo E-deficient mice. *Am. J. Transplant.* **3**, 562-569
8. Yu, Y., Yoon, S. O., Poulogiannis, G., Yang, Q., Ma, X. M., Villen, J., Kubica, N., Hoffman, G. R., Cantley, L. C., Gygi, S. P., and Blenis, J. (2011) Phosphoproteomic analysis identifies Grb10 as an mTORC1 substrate that negatively regulates insulin signaling. *Science* **332**, 1322-1326
9. Nakatsumi, H., Matsumoto, M., and Nakayama, K. I. (2017) Noncanonical Pathway for Regulation of CCL2 Expression by an mTORC1-FOXK1 Axis Promotes Recruitment of Tumor-Associated Macrophages. *Cell Rep.* **21**, 2471-2486
10. Hsu, P. P., Kang, S. A., Rameseder, J., Zhang, Y., Ottina, K. A., Lim, D., Peterson, T. R., Choi, Y., Gray, N. S., Yaffe, M. B., Marto, J. A., and Sabatini, D. M. (2011) The mTOR-regulated phosphoproteome reveals a mechanism of mTORC1-mediated inhibition of growth factor signaling. *Science* **332**, 1317-1322
11. He, L., Gomes, A. P., Wang, X., Yoon, S. O., Lee, G., Nagiec, M. J., Cho, S., Chavez, A., Islam, T., Yu, Y., Asara, J. M., Kim, B. Y., and Blenis, J. (2018)

mTORC1 Promotes Metabolic Reprogramming by the Suppression of GSK3-Dependent Foxk1 Phosphorylation. *Mol. Cell* **70**, 949-960 e944

12. Moens, C. B., and Selleri, L. (2006) Hox cofactors in vertebrate development. *Dev. Biol.* **291**, 193-206

13. Longobardi, E., Penkov, D., Mateos, D., De Florian, G., Torres, M., and Blasi, F. (2014) Biochemistry of the tale transcription factors PREP, MEIS, and PBX in vertebrates. *Dev. Dyn.* **243**, 59-75

14. Lin, J., Zhu, H., Hong, L., Tang, W., Wang, J., Hu, H., Wu, X., Chen, Y., Liu, G., Yang, Q., Li, J., Wang, Y., Lin, Z., Xiao, Y., Dai, W., Huang, M., Li, G., Li, A., Wang, J., Xiang, L., and Liu, S. (2021) Coexpression of HOXA6 and PBX2 promotes metastasis in gastric cancer. *Aging (Albany N. Y.)* **13**, 6606-6624

15. Qiu, Y., Morii, E., Tomita, Y., Zhang, B., Matsumura, A., Kitaichi, M., Okumura, M., and Aozasa, K. (2009) Prognostic significance of pre B cell leukemia transcription factor 2 (PBX2) expression in non-small cell lung carcinoma. *Cancer Sci.* **100**, 1198-1209

16. Qiu, Y., Song, B., Zhao, G., Deng, B., Makino, T., Tomita, Y., Wang, J., Luo, W., Doki, Y., Aozasa, K., and Morii, E. (2010) Expression level of Pre B cell leukemia homeobox 2 correlates with poor prognosis of gastric adenocarcinoma and esophageal squamous cell carcinoma. *Int. J. Oncol.* **36**, 651-663

17. Qiu, Y., Wang, Z. L., Jin, S. Q., Pu, Y. F., Toyosawa, S., Aozasa, K., and Morii, E. (2012) Expression level of pre-B-cell leukemia transcription factor 2 (PBX2) as a prognostic marker for gingival squamous cell carcinoma. *J Zhejiang Univ Sci B* **13**, 168-175

18. Harsha, C., Banik, K., Ang, H. L., Girisa, S., Vikkurthi, R., Parama, D., Rana, V., Shabnam, B., Khatoon, E., Kumar, A. P., and Kunnumakkara, A. B. (2020) Targeting AKT/mTOR in Oral Cancer: Mechanisms and Advances in Clinical Trials. *Int. J. Mol. Sci.* **21**

19. Hibdon, E. S., Razumilava, N., Keeley, T. M., Wong, G., Solanki, S., Shah, Y. M., and Samuelson, L. C. (2019) Notch and mTOR Signaling Pathways Promote Human Gastric Cancer Cell Proliferation. *Neoplasia* **21**, 702-712

20. Shi, N., Yu, H., and Chen, T. (2019) Inhibition of esophageal cancer growth through the suppression of PI3K/AKT/mTOR signaling pathway. *Onco Targets Ther.* **12**, 7637-7647

21. Tan, A. C. (2020) Targeting the PI3K/Akt/mTOR pathway in non-small cell lung cancer (NSCLC). *Thorac Cancer* **11**, 511-518
22. Tapia, O., Riquelme, I., Leal, P., Sandoval, A., Aedo, S., Weber, H., Letelier, P., Bellolio, E., Villaseca, M., Garcia, P., and Roa, J. C. (2014) The PI3K/AKT/mTOR pathway is activated in gastric cancer with potential prognostic and predictive significance. *Virchows Arch.* **465**, 25-33
23. Oshikawa, K., Matsumoto, M., Kodama, M., Shimizu, H., and Nakayama, K. I. (2020) A fail-safe system to prevent oncogenesis by senescence is targeted by SV40 small T antigen. *Oncogene* **39**, 2170-2186
24. He, L., Fei, D. L., Nagiec, M. J., Mutvei, A. P., Lamprakis, A., Kim, B. Y., and Blenis, J. (2019) Regulation of GSK3 cellular location by FRAT modulates mTORC1-dependent cell growth and sensitivity to rapamycin. *Proc. Natl. Acad. Sci. U. S. A.* **116**, 19523-19529
25. Nakatsumi, H., Oka, T., Higa, T., Shirane, M., and Nakayama, K. I. (2018) Nuclear-cytoplasmic shuttling protein PP2A(B56) contributes to mTORC1-dependent dephosphorylation of FOXK1. *Genes Cells* **23**, 599-605
26. Berman, A. J., Thoreen, C. C., Dedeic, Z., Chettle, J., Roux, P. P., and Blagden, S. P. (2021) Controversies around the function of LARP1. *RNA Biol.* **18**, 207-217
27. Kinoshita, E., Kinoshita-Kikuta, E., Takiyama, K., and Koike, T. (2006) Phosphate-binding tag, a new tool to visualize phosphorylated proteins. *Mol Cell Proteomics* **5**, 749-757
28. Ota, T., Asahina, H., Park, S. H., Huang, Q., Minegishi, T., Auersperg, N., and Leung, P. C. (2008) HOX cofactors expression and regulation in the human ovary. *Reprod. Biol. Endocrinol.* **6**, 49
29. Betz, C., and Hall, M. N. (2013) Where is mTOR and what is it doing there? *J. Cell Biol.* **203**, 563-574
30. Oh, W. J., and Jacinto, E. (2011) mTOR complex 2 signaling and functions. *Cell Cycle* **10**, 2305-2316
31. Rebelo, S., Santos, M., Martins, F., da Cruz e Silva, E. F., and da Cruz e Silva, O. A. (2015) Protein phosphatase 1 is a key player in nuclear events. *Cell. Signal.* **27**, 2589-2598
32. Korrodi-Gregorio, L., Esteves, S. L., and Fardilha, M. (2014) Protein phosphatase 1 catalytic isoforms: specificity toward interacting proteins. *Transl. Res.* **164**, 366-

391

33. Evangelisti, C., Chiarini, F., Paganelli, F., Marmiroli, S., and Martelli, A. M. (2020) Crosstalks of GSK3 signaling with the mTOR network and effects on targeted therapy of cancer. *Biochim Biophys Acta Mol Cell Res* **1867**, 118635

34. Bautista, S. J., Boras, I., Vissa, A., Mecica, N., Yip, C. M., Kim, P. K., and Antonescu, C. N. (2018) mTOR complex 1 controls the nuclear localization and function of glycogen synthase kinase 3beta. *J. Biol. Chem.* **293**, 14723-14739

35. Hoermann, B., and Kohn, M. (2021) Evolutionary crossroads of cell signaling: PP1 and PP2A substrate sites in intrinsically disordered regions. *Biochem. Soc. Trans.* **49**, 1065-1074

36. Brautigan, D. L., and Shenolikar, S. (2018) Protein Serine/Threonine Phosphatases: Keys to Unlocking Regulators and Substrates. *Annu. Rev. Biochem.* **87**, 921-964

37. Li, Q., Zhao, Q., Zhang, J., Zhou, L., Zhang, W., Chua, B., Chen, Y., Xu, L., and Li, P. (2019) The Protein Phosphatase 1 Complex Is a Direct Target of AKT that Links Insulin Signaling to Hepatic Glycogen Deposition. *Cell Rep.* **28**, 3406-3422 e3407

Figure Legends

Fig. 1. Identification of PBX2 as a downstream effector of mTORC1. (A) Scheme for the acquisition of phosphoproteomics data in our previous study (9). Serum-deprived HeLa cells were exposed to 10 nM rapamycin or 10 μM U0126 for 30 min before stimulation with serum for 20 min. Alternatively, HeLa cells were either deprived of serum for 16 h before stimulation with insulin for the indicated times or deprived of amino acids for 5 h before stimulation with amino acids for the indicated times. (B) Venn diagram showing the overlap in proteins found to undergo dephosphorylation in response to serum in a rapamycin-sensitive manner (but not in a U0126-sensitive manner) or in response to insulin or amino acid stimulation in a time-dependent manner (left panel). The overlap in the dephosphorylation sites for the 11 proteins found to be dephosphorylated under all three conditions is also shown (right panel).

Fig. 2. mTORC1-dependent dephosphorylation of PBX2. (A) Serum-deprived 3T3-L1 cells were incubated with 10 nM rapamycin, 100 nM Torin 1, or 0.1% dimethyl sulfoxide (DMSO, vehicle) for 1 h and then in the additional presence of 100 nM insulin for the indicated times, after which cell extracts were subjected to SDS-PAGE with or without Phos-Tag followed by immunoblot (IB) analysis with antibodies to the indicated total or phosphorylated (p-) proteins. Phosphorylation of p70 S6 kinase (S6K), S6, and 4E-BP1 was examined to monitor mTORC1 activity. (B) Serum-deprived 3T3-L1 cells infected with retroviruses encoding HA epitope–tagged PBX1, PBX2, PBX3, or PBX4 were incubated with 10 nM rapamycin, 100 nM Torin 1, or 0.1% DMSO for 1 h and then in the additional absence or presence of 100 nM insulin for 30 min, after which cell extracts were analyzed as in (A). HSP90 was examined as a loading control.

Fig. 3. Ser^{330} of PBX2 is dephosphorylated in the nucleus in an mTORC1-dependent manner. (A) Serum-deprived 3T3-L1 cells infected with retroviruses encoding HA epitope–tagged WT or mutant (S330A or S330D) forms of PBX2 were incubated with 10 nM rapamycin or 100 nM Torin 1 for 1 h and then in the additional absence or presence of 100 nM insulin for 30 min, after which cell extracts were subjected to SDS-PAGE with or without Phos-tag followed by immunoblot analysis with antibodies to the indicated proteins. (B–D) Immunocytofluorescence analysis of

the HA epitope (green) in 3T3-L1 cells expressing HA-tagged WT or mutant (S330A, S330D, or S330E) forms of PBX2 (B), in 3T3-L1 cells expressing HA-PBX2(WT) and incubated with or without 10 nM rapamycin or 100 nM Torin 1 for 1 h (C), or in 3T3-L1 cells expressing HA-PBX2(WT) that were deprived of serum and then incubated with 100 nM insulin for the indicated times (D). Nuclei were stained with DAPI (blue). Scale bars, 10 μm.

Fig. 4. mTORC1 regulates PBX2 phosphorylation through GSK3. (A and B) Serum-deprived 3T3-L1 cells were incubated with various inhibitors [Torin1 (100 nM), staurosporine (10, 100 nM, and 1 μM), LY294002 (100 nM, 1 and 10 μM), AktVIII (100 nM, 1 and 10 μM), Go6983 (10, 100 nM and 1 μM), AZD6244 (10, 100 nM, and 1 μM), SB203580 (100 nM, 1 and 10 μM), or SB216763 (100 nM, 1 and 10 μM)] for 10 min and then in the additional absence or presence of 100 nM insulin for 20 min, after which cell extracts were subjected to SDS-PAGE with or without Phos-tag followed by immunoblot analysis with antibodies to the indicated proteins. Phosphorylation of ERK1/2 and MAPKAPK-2 was examined to monitor inhibition of MEK (AZD6244) and p38 mitogen-activated protein kinase (SB203580), respectively. (C) Serum-deprived 3T3-L1 cells expressing GSK3α, GSK3β, or control shRNAs were incubated with Torin1 (100 nM) or CHIR99021 (1 μM) for 10 min and then in the additional absence or presence of 100 nM insulin for 25 min, after which cell extracts were subjected to analysis as in (A) and (B). (D) Immunofluorescence analysis of GSK3 (green) in serum-deprived 3T3-L1 cells incubated with or without 10 nM rapamycin or 100 nM Torin 1 for 1 h and then in the additional absence or presence of 100 nM insulin for 30 min. Nuclei were stained with DAPI (blue). Scale bars, 20 μm.

Fig. 5. PP1 dephosphorylates PBX2 at Ser^{330}. (A) Serum-deprived 3T3-L1 cells were incubated with calyculin A (0, 5, 10 or 50 nM) for 10 min and then in the additional absence or presence of 100 nM insulin for 20 min, after which cell extracts were subjected to SDS-PAGE with or without Phos-tag followed by immunoblot analysis with antibodies to the indicated proteins. (B) Serum-deprived HeLa cells that had been transfected with a control siRNA or siRNAs specific for the catalytic subunits of PP1 or PP2A were stimulated with 100 nM insulin for 20 min, after which cell extracts were analyzed as in (A). (C) Quantification of the Ser^{330}-phosphorylated/Ser^{330}-

dephosphorylated band intensity ratio for PBX2 relative to that of siControl cells for immunoblots as in (B). Data are means ± SEM from three independent experiments. *P < 0.05, **P < 0.01 (Dunnett's test). (D) Immunocytofluorescence analysis of PP1 (green) in serum-deprived 3T3-L1 cells incubated with or without 10 nM rapamycin or 100 nM Torin 1 for 1 h and in the additional absence or presence of 100 nM insulin for 30 min. Nuclei were stained with DAPI (blue). Scale bars, 20 μm.

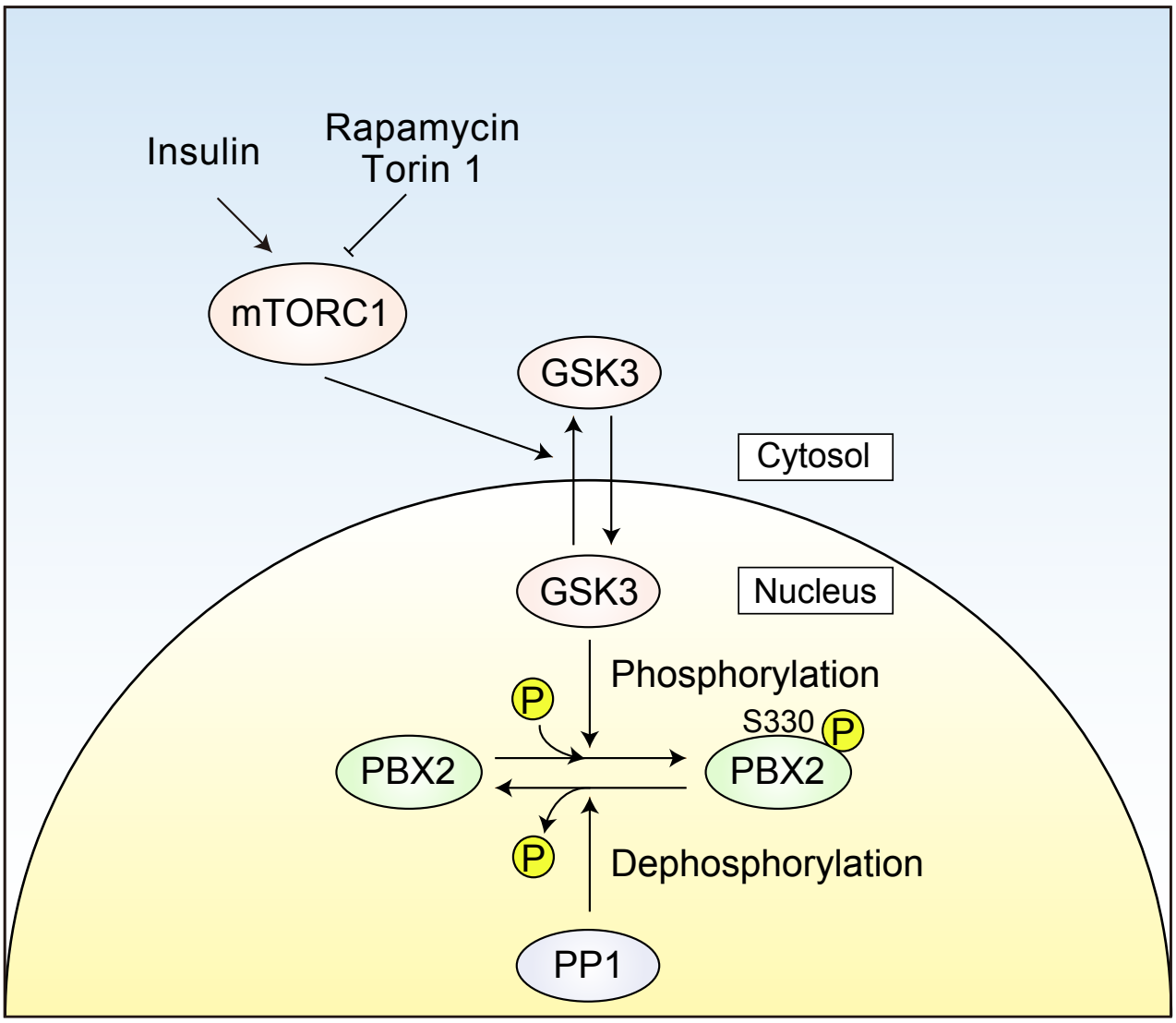

Wada et al. Graphical abstract

A

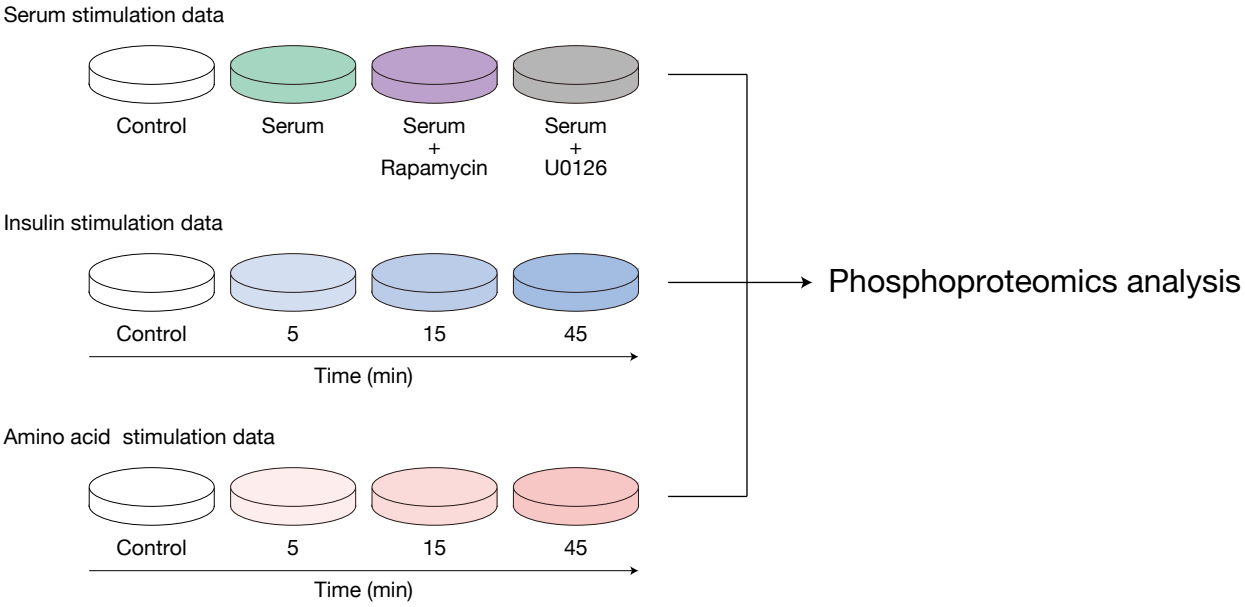

B

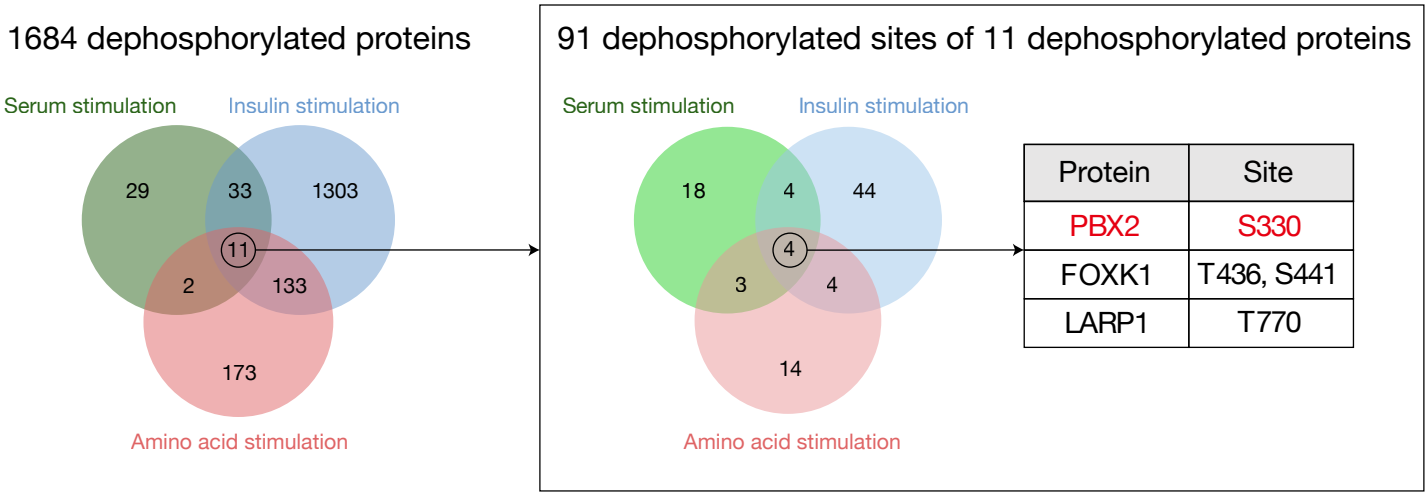

Protein	Site
PBX2	S330
FOXK1	T436, S441
LARP1	T770

Wada et al. Figure 1

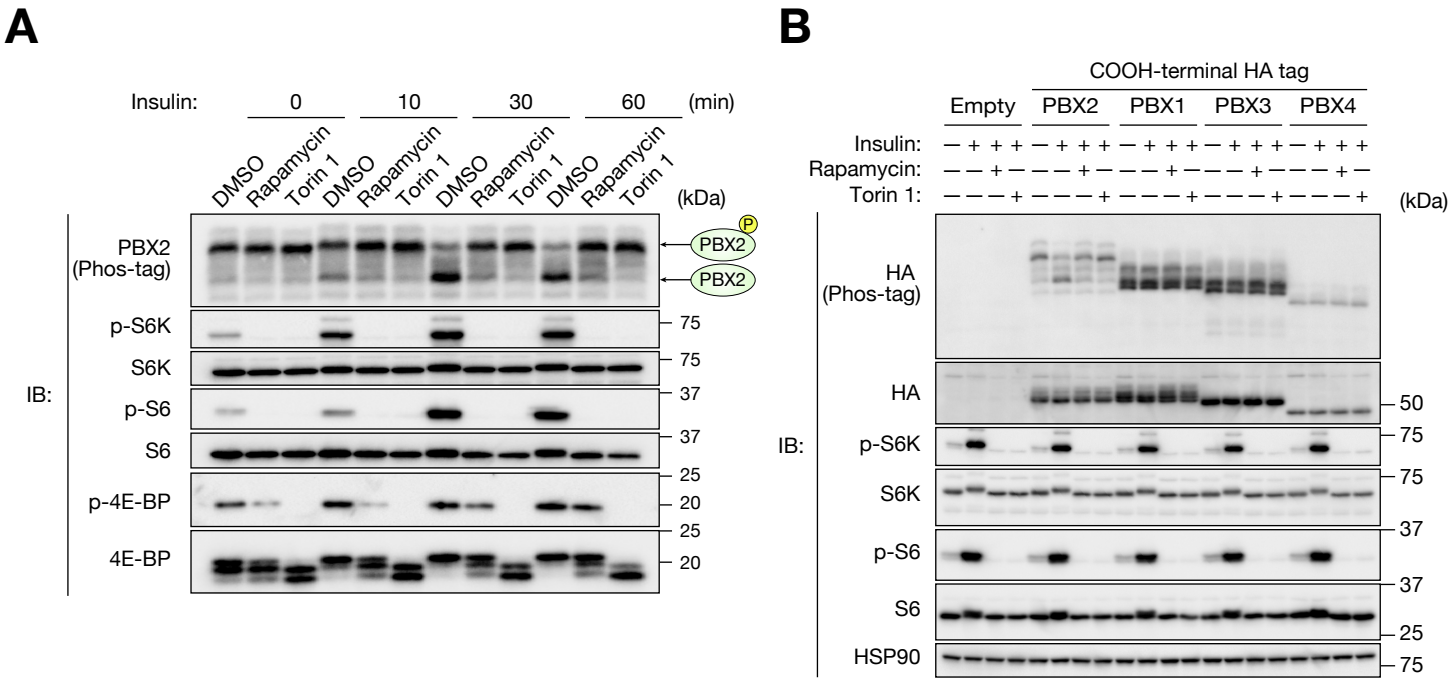

Wada et al. Figure 2

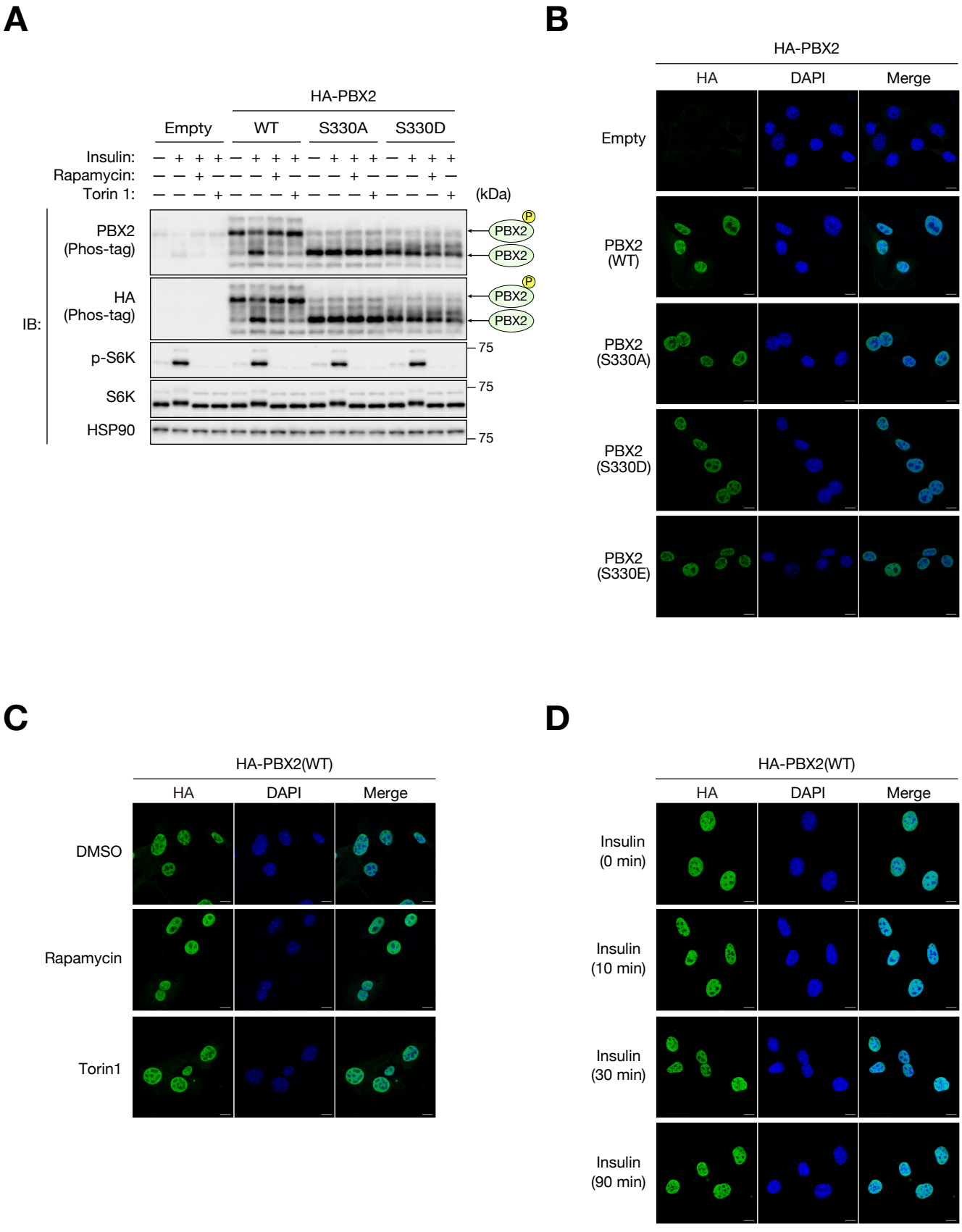

Wada et al. Figure 3

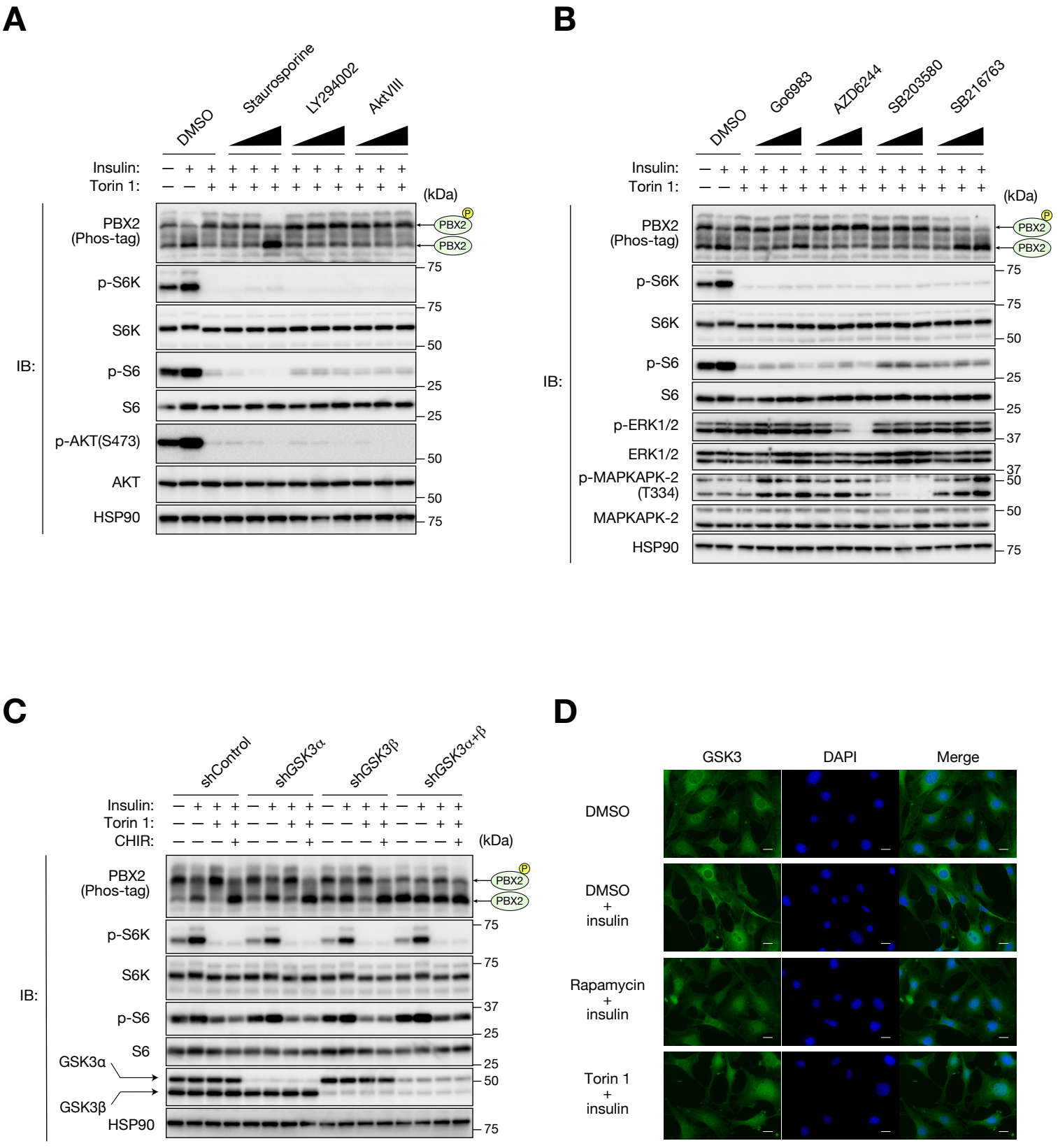

Wada et al. Figure 4

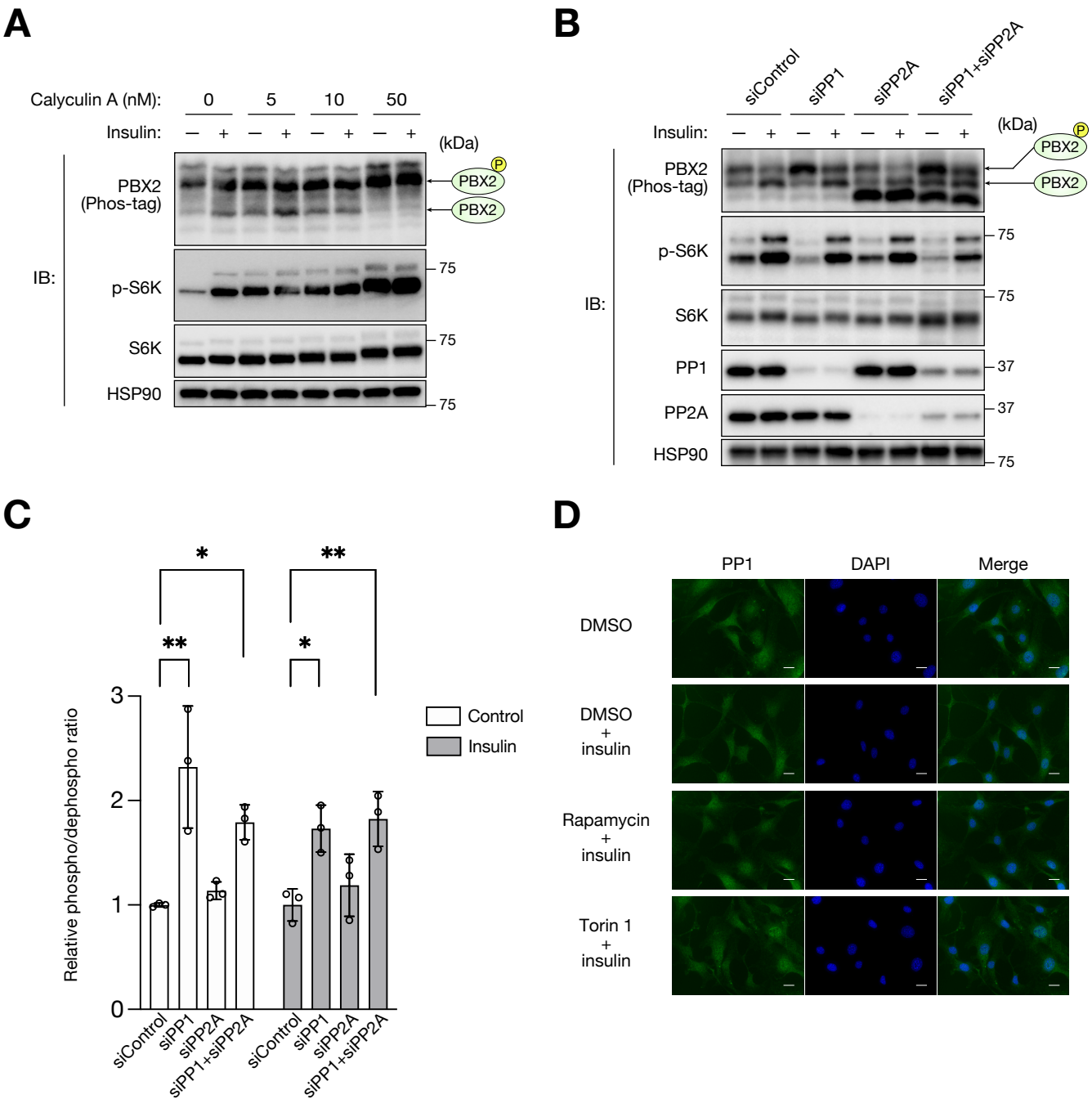

Wada et al. Figure 5